Frequency Corrections in Flux Computations

Xinhua Zhou, Ph.D., Senior Scientist

Eddy sizes, speed, and frequency

$$\text{Period}(\tau) = \frac{\text{Wavelength}\,(\lambda)}{\text{Wind speed}\,(U)} = \frac{1}{\text{Frequency}\,(f)}$$

$$f = \frac{U}{\lambda}$$

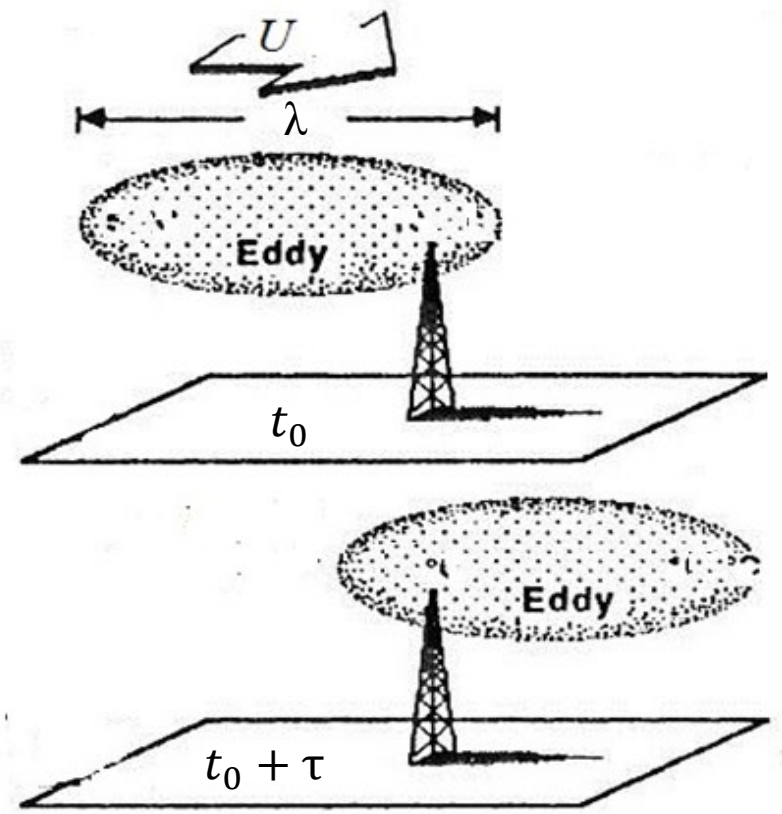

Measuring CO_2 for the same air flow by two gas analyzers with different path lengths

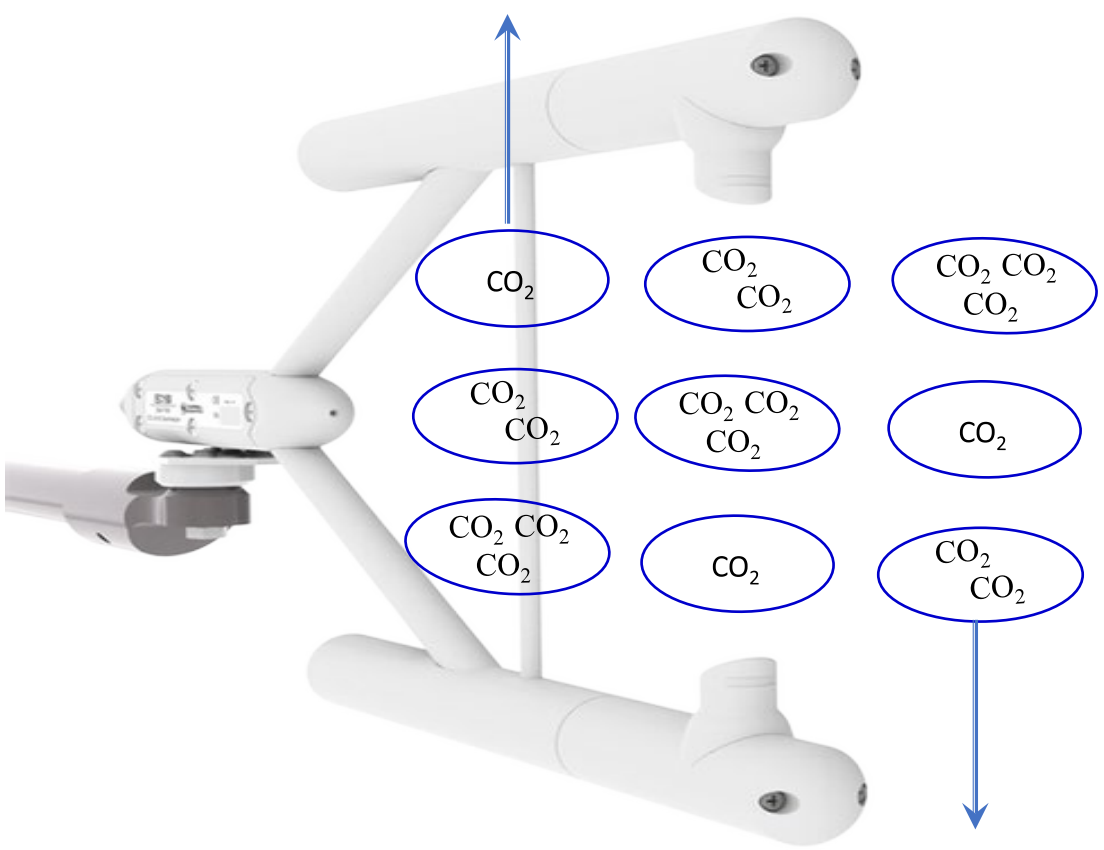

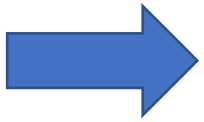

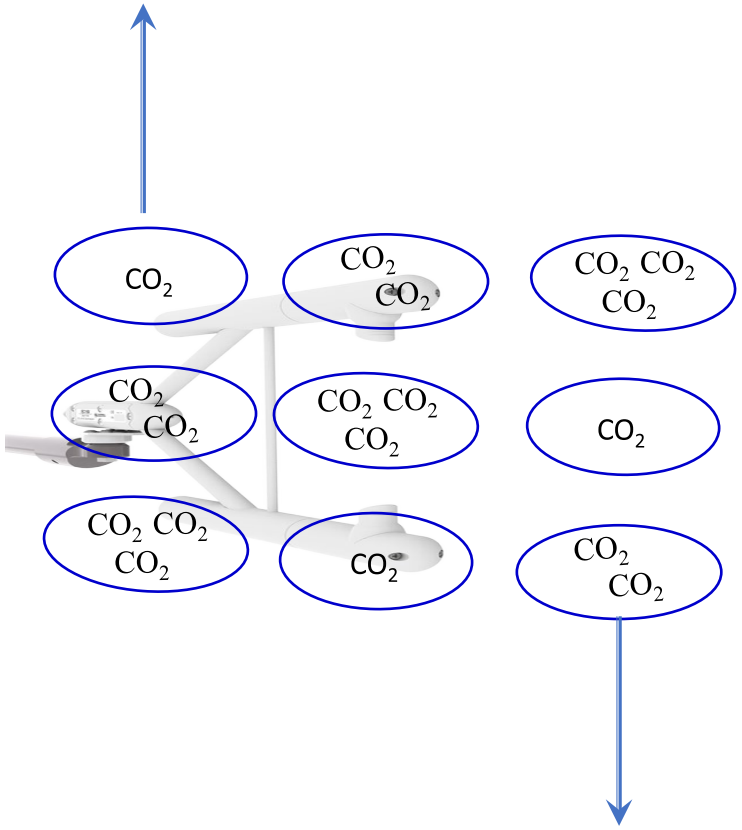

CO_2 (ρ_{CO_2} in molCO_2 m^{-3})	2	2	2	$F_c = \overline{\rho'_{CO_2} w'}$ [a]	2	3	1	$F_c = \overline{\rho'_{CO_2} w'}$ [a]
Vertical wind (w in m s^{-1})	$\overline{w}+1$	$\overline{w}$	$\overline{w}-1$		$\overline{w}+1$	$\overline{w}$	$\overline{w}-1$	
$\overline{\rho'_{CO_2} w'}$ (molCO_2 m^{-2} s^{-1})	0	0	0	0	0	0	+1	+1

[a] Air density is assumed to be a constant.

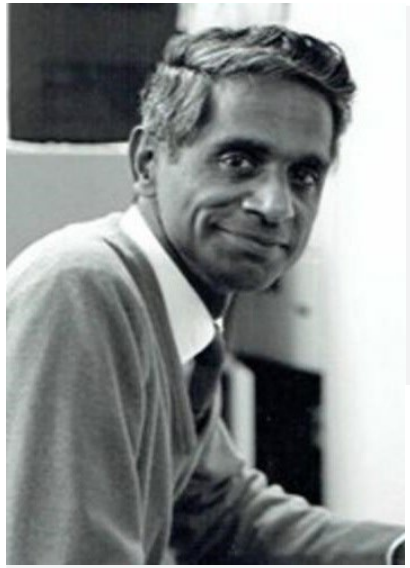

551.524.4 : 551.551.8 : 517.512.2

The effect of vertical line averaging on the spectra of temperature and heat-flux

By J. C. KAIMAL,
Air Force Cambridge Research Laboratories, Bedford, Massachusetts

1968. Quart. J. Roy. Meteor Soc. 94: 149–165.

(Manuscript received 30 June 1967; in revised form 13 November 1967)

SUMMARY

The paper describes an attempt to evaluate the effects of vertical line averaging on temperature statistics by using simultaneous measurements from sensors of different lengths. Results show that the transfer function for vertical line averaging derived by Gurvich for the vertical velocity component applies also to temperature spectra. Heat-flux, when computed with vertical velocity measurements from a sonic anemometer, is relatively insensitive to line averaging (at least up to 80 cm at 9 m height). But the coherence between the line average and its mid-point value shows consistent behaviour only for short line lengths of the order of 20 cm. With longer lengths the coherence is likely to vary from one run to another depending on mean wind speed.

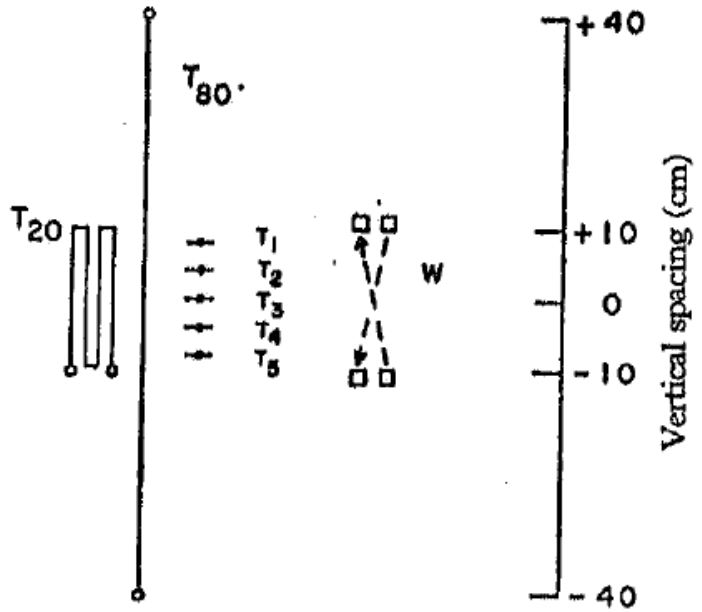

T_{20} 20 cm average (Plat. wire)
T_{80} 80 cm average (Plat. wire)
T_1-T_5 Point measurements (Thermistors)
W vertical velocity (sonic)

Figure 1. Diagram of sensor placement for the experiment.

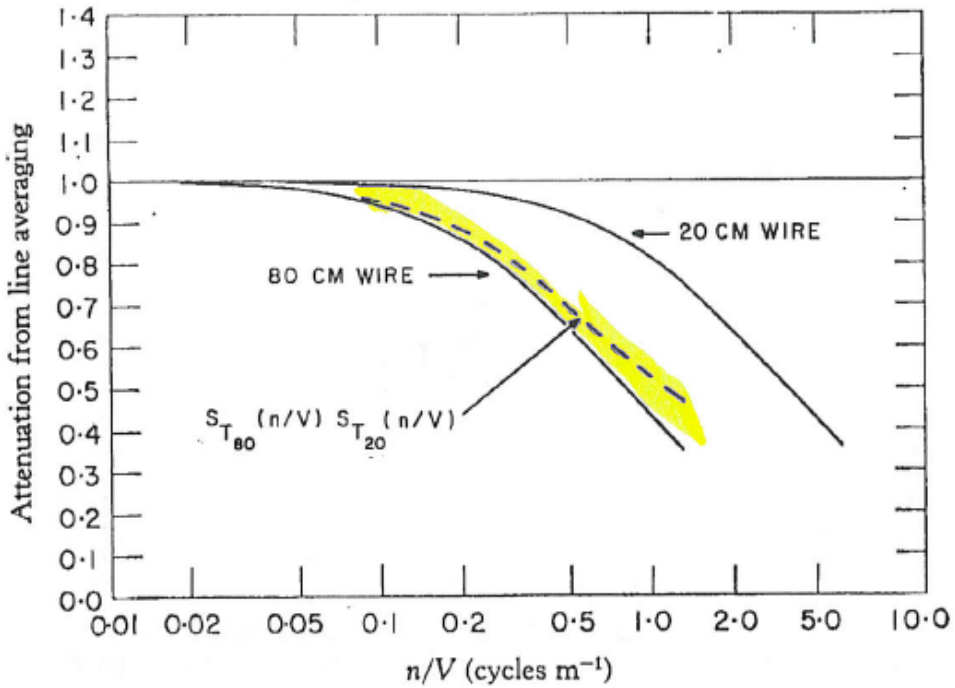

Figure 3. Theoretical attenuation curves for 20- and 80-cm line averaging. Relative attenuation between the two is indicated by dashed curves.

Kaimal, J.C. 1968. The effect of vertical line averaging on the spectra of temperature and heat-flux, Qaurt. J. Roy. Meteor. Soc. 94: 149-155.

Implication of time constant (τ) in physics

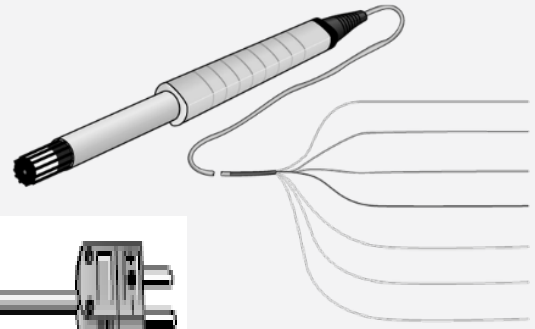

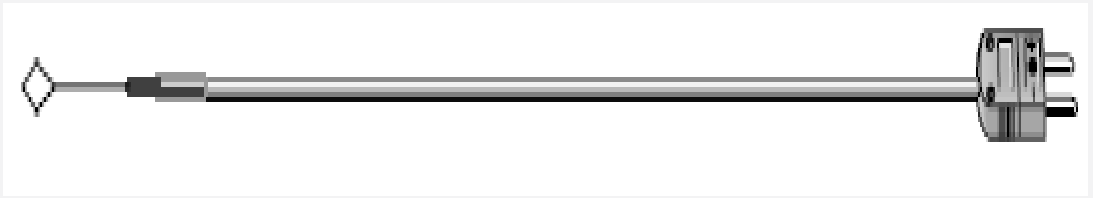

Moore (1986)

$$\tau = \gamma D^2 \frac{\rho_a C}{k_a \mathbf{Nu}}$$

γ	Shape factor
D	Dimension
ρ_a	Material density of sensor sensing component
C	Specific heat of materials for sensor sensing
k_a	Thermal conductivity of air
Nu	Nusselt number

Moore, C.J., 1986. Frequency response corrections for eddy correlation systems, Boundary-Layer Meteorol. 37: 17-35.

Response of temperature sensor as described in terms of time constant

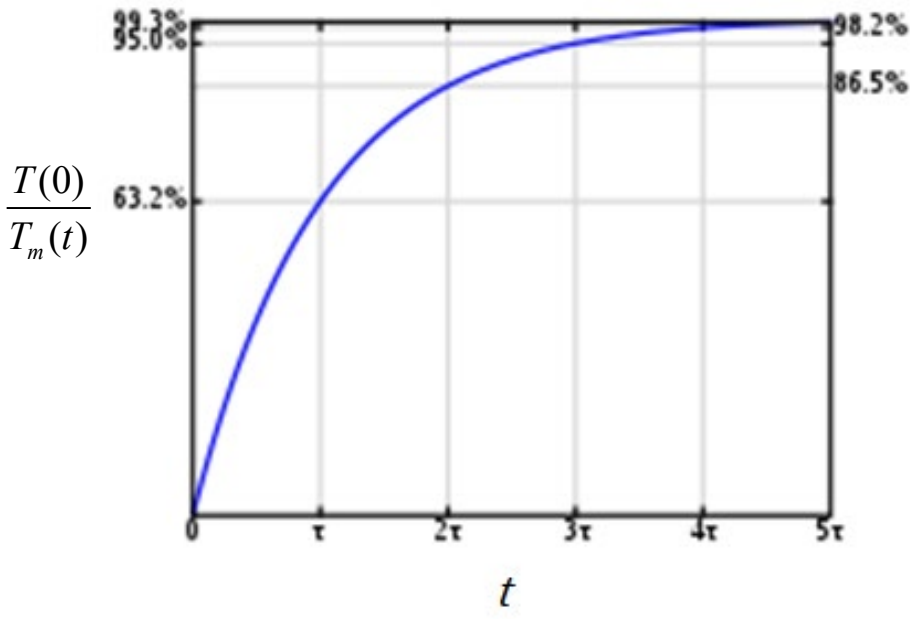

$$\frac{dT_m(t)}{dt} = \frac{T(t) - T_m(t)}{\tau}$$

t	Time
$T(t)$	Tempearture of media at t
$T_m(t)$	Temperature measured at t
τ	Time constant

Burt and Podesta (2020)

Burt, S., M.d. Podesta. 2020. Response times of meteorological air temperature sensors, Q J R Meteorol Soc, 146: 2789-2800.

Response time of sensors

Campbell Scientific sonic anemometer thermometry

(CSAT, Campbell Scientific Inc., UT, USA)

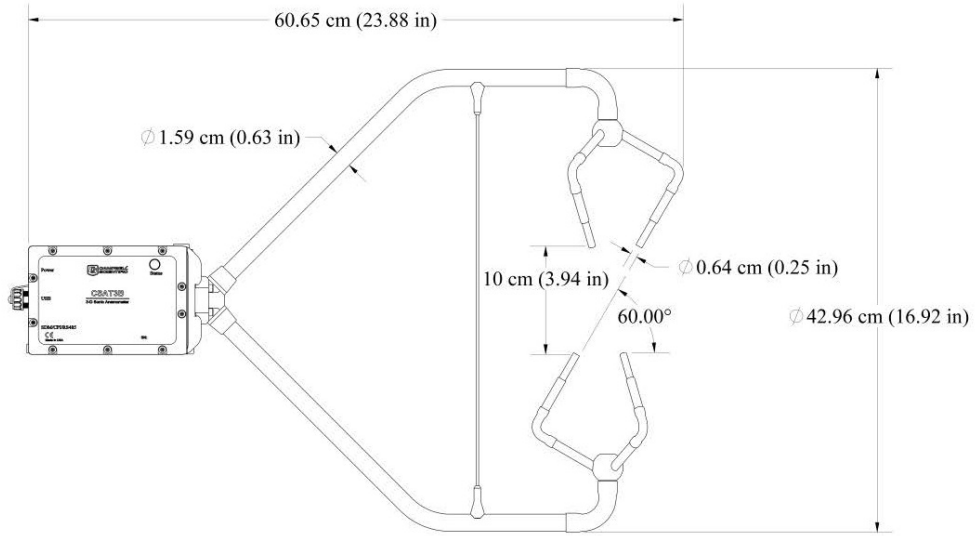

$$\text{Response time}^{a} = \frac{\text{Path length (11.54 cm)}}{\text{Speed of sound - flow speed along the path}}$$

$$\approx 3.6\times10^{-4}\,\text{s}$$

Infrared CO_2-H_2O analyzer

(EC150, Campbell Scientific Inc., UT, USA)

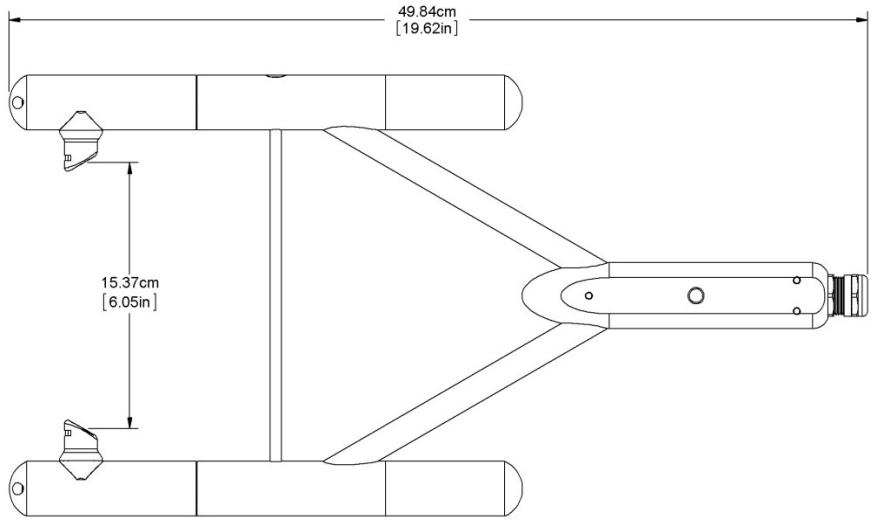

$$\text{Response time}^{a} = \frac{\text{Path length}}{\text{Speed of light}}$$

$$\approx 5.1\times10^{-10}\,\text{s}$$

[a] Electronic response is assumed to be instantaneous.

Frequency loss due to sensor separation

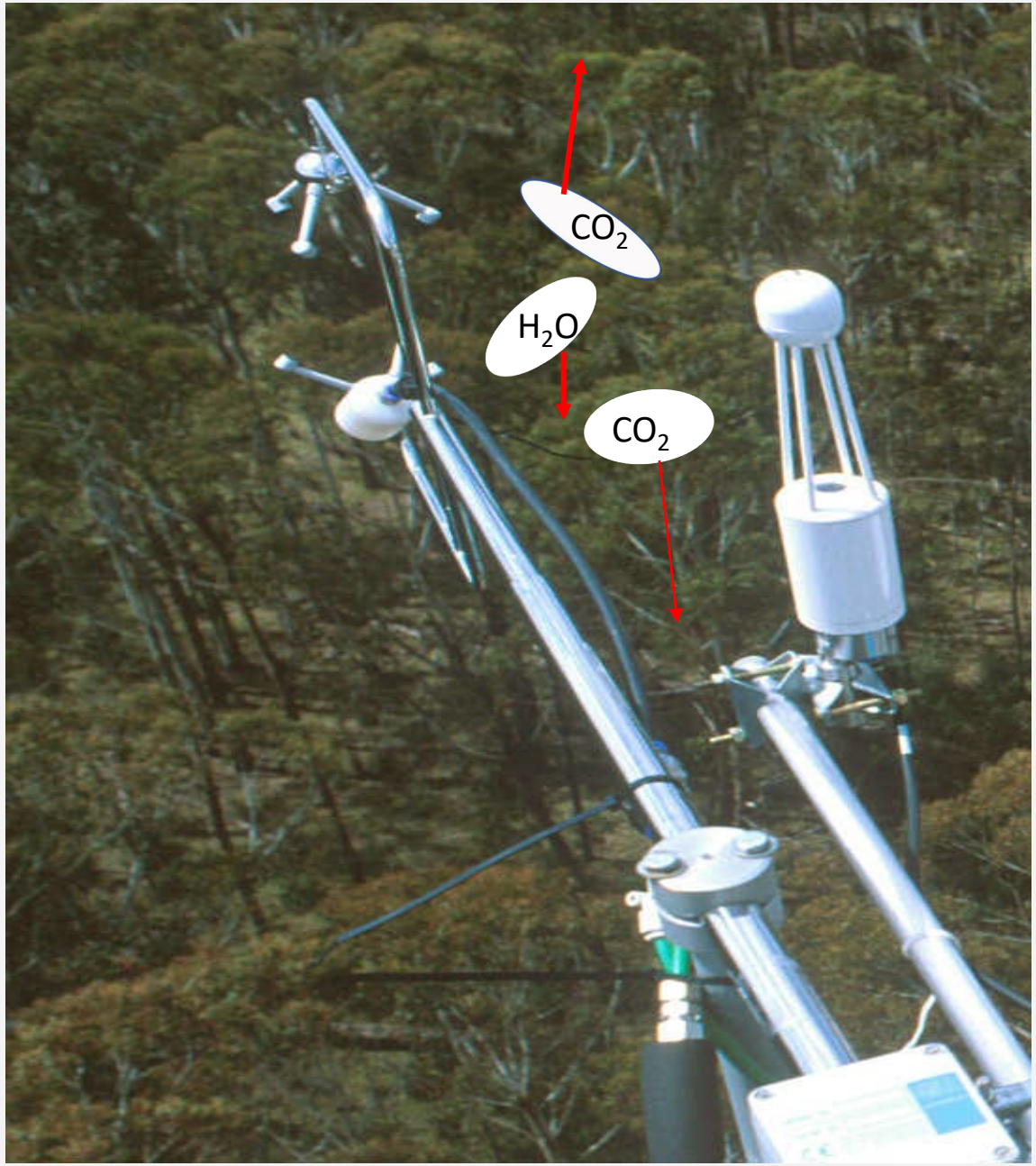

Low frequency loss due to block averaging in flux computations

CO_2 $$F_{CO_2} = \rho_d \overline{w'\chi'}_{CO_2}$$ (e.g., $w' = w - \bar{w}$)

H_2O $$FH_{2O} = \rho_d \overline{w'\chi'}_{H_2O}$$

Summary for frequency losses

High frequency

a. Line averaging.

b. Delay in response to measured variables.

c. Spatial separation between sensors

Low frequency

a. Block averaging.

Any variable measured in an eddy-covariance system is a time series (i.e., a function of time).

For frequency corrections, this time series in a time domain needs to be transformed into a frequency domain.

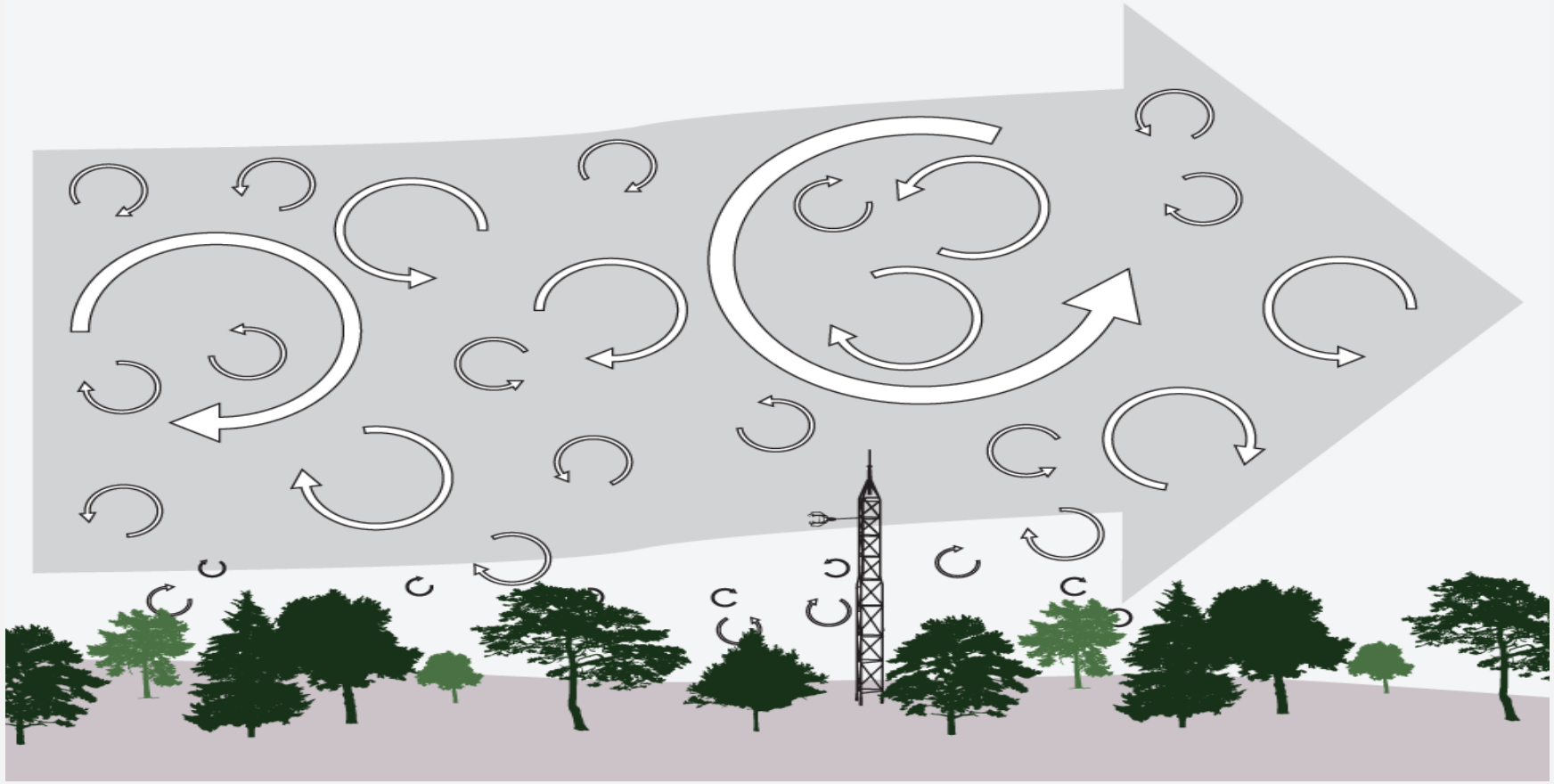

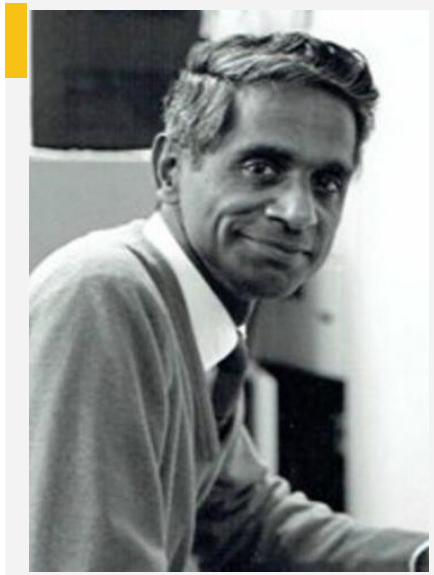

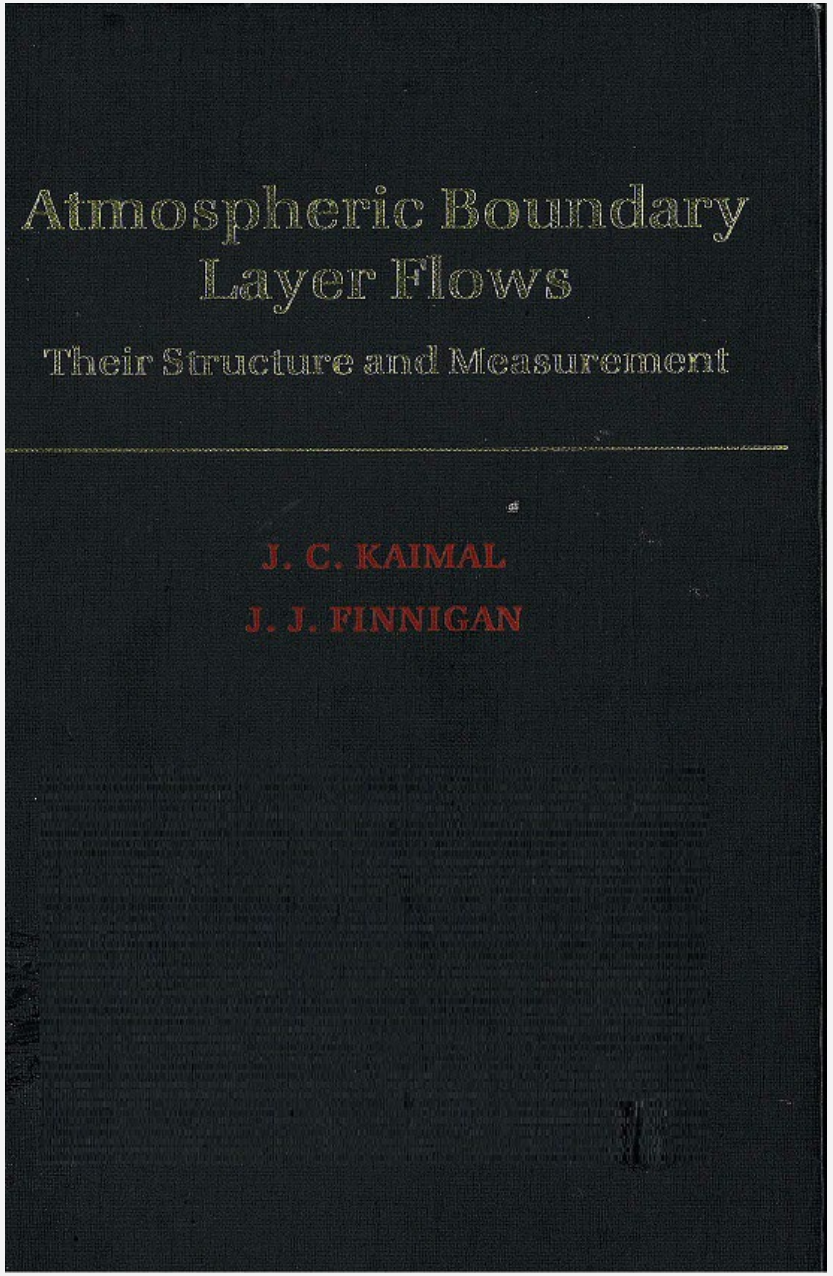

Kaimal, JC, JJ Finnigan. 1994. Atmospheric Boundary Layer Flows: Their Structure and Measurement. Oxford University Press, Oxford, 289 p.

Vertical wind (w) measured in a time domain to a frequency domain

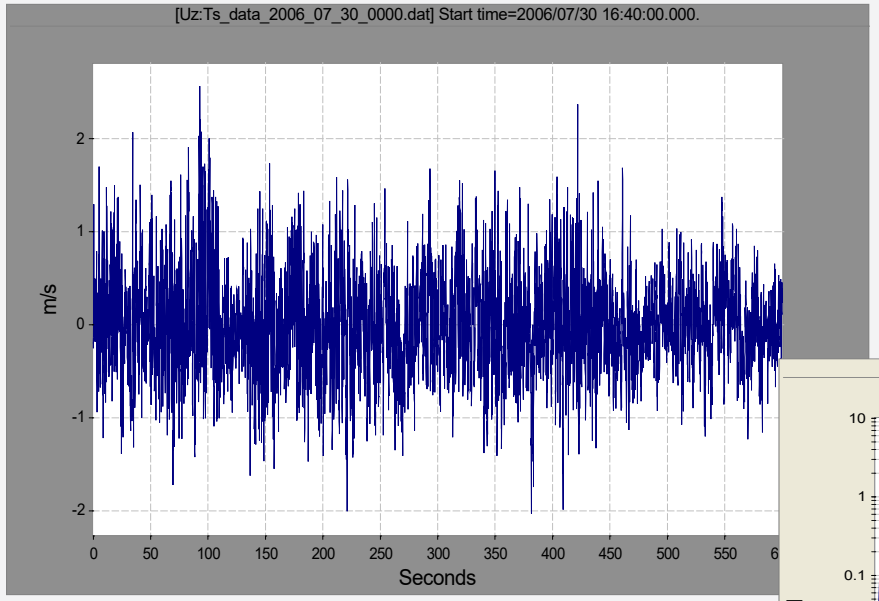

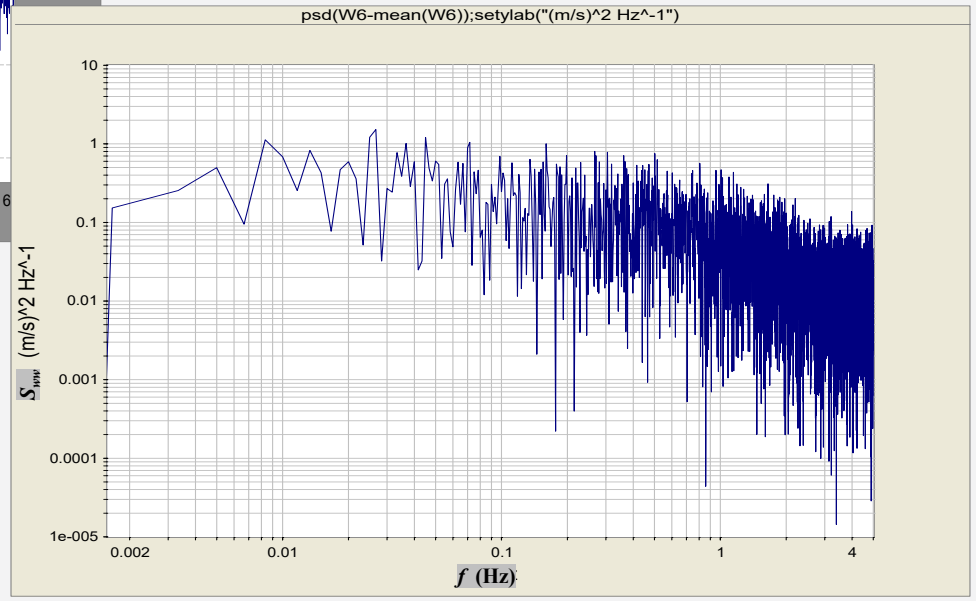

Smoothed power spectrum of vertical wind speed

$$\overline{w'w'} = \int_0^{+\infty} S_{ww}(f)\,df$$

Kaimal &Finnigan (1994)

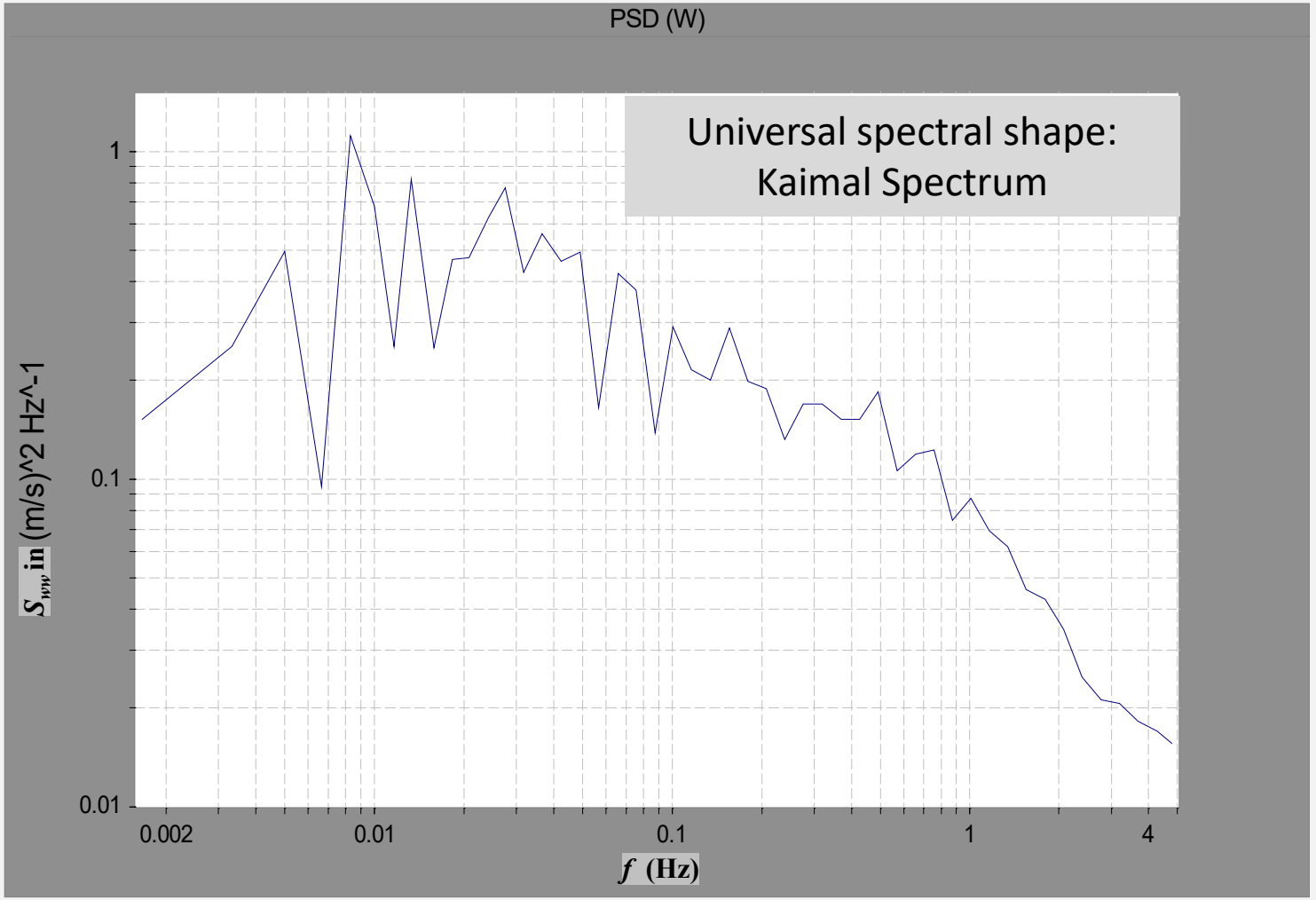

Kaimal, JC, JJ Finnigan. 1994. Atmospheric Boundary Layer Flows: Their Structure and Measurement, Oxford University Press, New York, 289 p.

Relationship of cospectrum to a flux

$$\overline{\alpha' w'} = \int_{-\infty}^{+\infty} S_{\alpha w}(f)\,df$$

Pages 57 to 61 in Kaimal & Finnigan (1994)

α represents u, v, T, T_s, ρ_{CO_2}, χ_{CO_2}, ρ_{H_2O}, χ_{H_2O},

OR other gas species amount.

Normalized cospectrum

$$S_{\alpha w}(f)_N = \frac{S_{\alpha w}(f)_T}{(\alpha' w')_T}$$

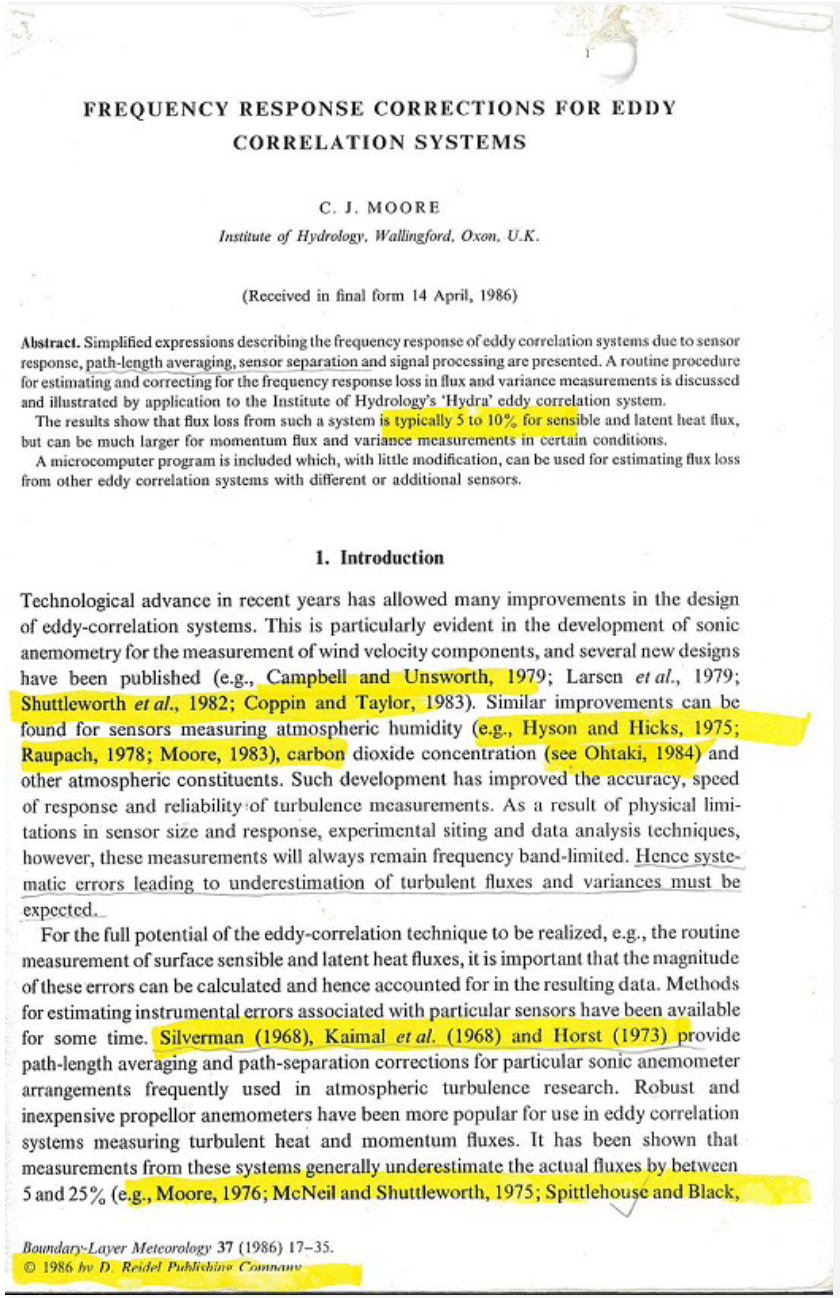

FREQUENCY RESPONSE CORRECTIONS FOR EDDY CORRELATION SYSTEMS

C. J. MOORE

Institute of Hydrology, Wallingford, Oxon, U.K.

(Received in final form 14 April, 1986)

Abstract. Simplified expressions describing the frequency response of eddy correlation systems due to sensor response, path-length averaging, sensor separation and signal processing are presented. A routine procedure for estimating and correcting for the frequency response loss in flux and variance measurements is discussed and illustrated by application to the Institute of Hydrology's 'Hydra' eddy correlation system.

The results show that flux loss from such a system is typically 5 to 10% for sensible and latent heat flux, but can be much larger for momentum flux and variance measurements in certain conditions.

A microcomputer program is included which, with little modification, can be used for estimating flux loss from other eddy correlation systems with different or additional sensors.

1. Introduction

Technological advance in recent years has allowed many improvements in the design of eddy-correlation systems. This is particularly evident in the development of sonic anemometry for the measurement of wind velocity components, and several new designs have been published (e.g., Campbell and Unsworth, 1979; Larsen *et al.*, 1979; Shuttleworth *et al.*, 1982; Coppin and Taylor, 1983). Similar improvements can be found for sensors measuring atmospheric humidity (e.g., Hyson and Hicks, 1975; Raupach, 1978; Moore, 1983), carbon dioxide concentration (see Ohtaki, 1984) and other atmospheric constituents. Such development has improved the accuracy, speed of response and reliability of turbulence measurements. As a result of physical limitations in sensor size and response, experimental siting and data analysis techniques, however, these measurements will always remain frequency band-limited. Hence systematic errors leading to underestimation of turbulent fluxes and variances must be expected.

For the full potential of the eddy-correlation technique to be realized, e.g., the routine measurement of surface sensible and latent heat fluxes, it is important that the magnitude of these errors can be calculated and hence accounted for in the resulting data. Methods for estimating instrumental errors associated with particular sensors have been available for some time. Silverman (1968), Kaimal *et al.* (1968) and Horst (1973) provide path-length averaging and path-separation corrections for particular sonic anemometer arrangements frequently used in atmospheric turbulence research. Robust and inexpensive propellor anemometers have been more popular for use in eddy correlation systems measuring turbulent heat and momentum fluxes. It has been shown that measurements from these systems generally underestimate the actual fluxes by between 5 and 25% (e.g., Moore, 1976; McNeil and Shuttleworth, 1975; Spittlehouse and Black,

Boundary-Layer Meteorology **37** (1986) 17–35.

Moore CJ. 1986.
Frequency response corrections for eddy correlation systems.
Bound-Layer Meteorol 37: 17-35.

Normalized Cospectra

$$\frac{z}{L} > 0$$

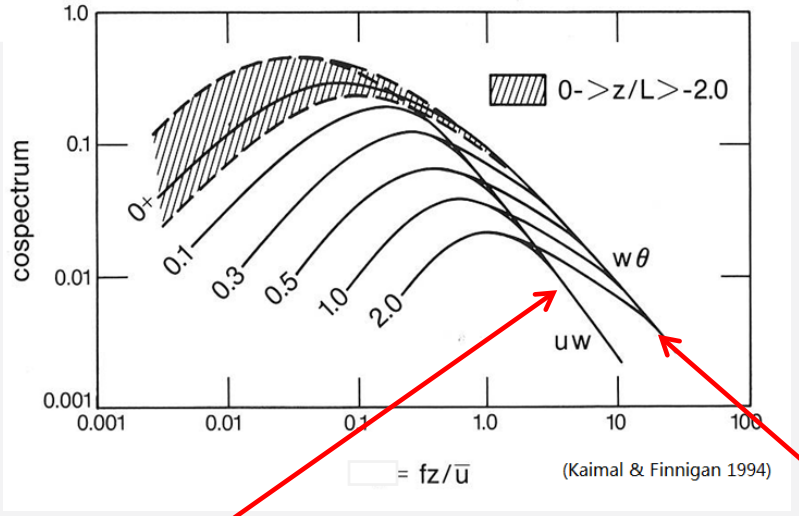

Vertical with horizontal wind

$$fS_{uw}(f)_N = \frac{fz/\bar{u}}{A_{uw} + B_{uw}\left(\frac{fz}{\bar{u}}\right)^{2.1}}$$

$$A_{uw} = 0.124\left(1 + 7.9\frac{z}{L}\right)^{0.75}$$

$$B_{uw} = 23.252\left(1 + 7.9\frac{z}{L}\right)^{-0.825}$$

Vertical wind with air temperature

$$fS_{Tw}(f)_N = \frac{fz/\bar{u}}{A_{Tw} + B_{Tw}\left(\frac{fz}{\bar{u}}\right)^{2.1}}$$

$$A_{Tw} = 0.284\left(1 + 6.4\frac{z}{L}\right)^{0.75}$$

$$B_{Tw} = 9.3447\left(1 + 6.4\frac{z}{L}\right)^{-0.825}$$

Normalized Cospectra

$$\frac{z}{L} \le 0$$

Vertical with horizontal wind

$$fS_{uw}(f)_N = \begin{cases} \dfrac{20.78\, fz/\bar{u}}{\left(1+\dfrac{31z}{\bar{u}}f\right)^{1.575}} & \dfrac{z}{\bar{u}}f < 0.24 \\ \dfrac{12.66\, fz/\bar{u}}{\left(1+\dfrac{9.6z}{\bar{u}}f\right)^{2.4}} & \dfrac{z}{\bar{u}}f \ge 0.24 \end{cases}$$

Vertical wind with air temperature

$$fS_{Tw}(f)_N = \begin{cases} \dfrac{12.92\, fz/\bar{u}}{\left(1+\dfrac{26.7z}{\bar{u}}f\right)^{1.375}} & \dfrac{z}{\bar{u}}f < 0.54 \\ \dfrac{4.378\, fz/\bar{u}}{\left(1+\dfrac{3.8z}{\bar{u}}f\right)^{2.4}} & \dfrac{z}{\bar{u}}f \ge 0.54 \end{cases}$$

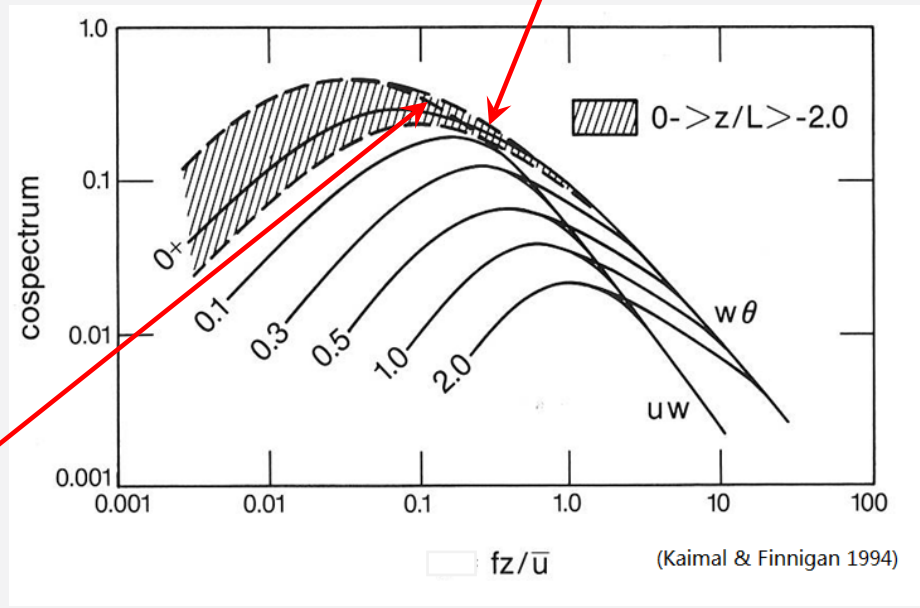

Cospectrum from an ideal vs. non-idea measurement

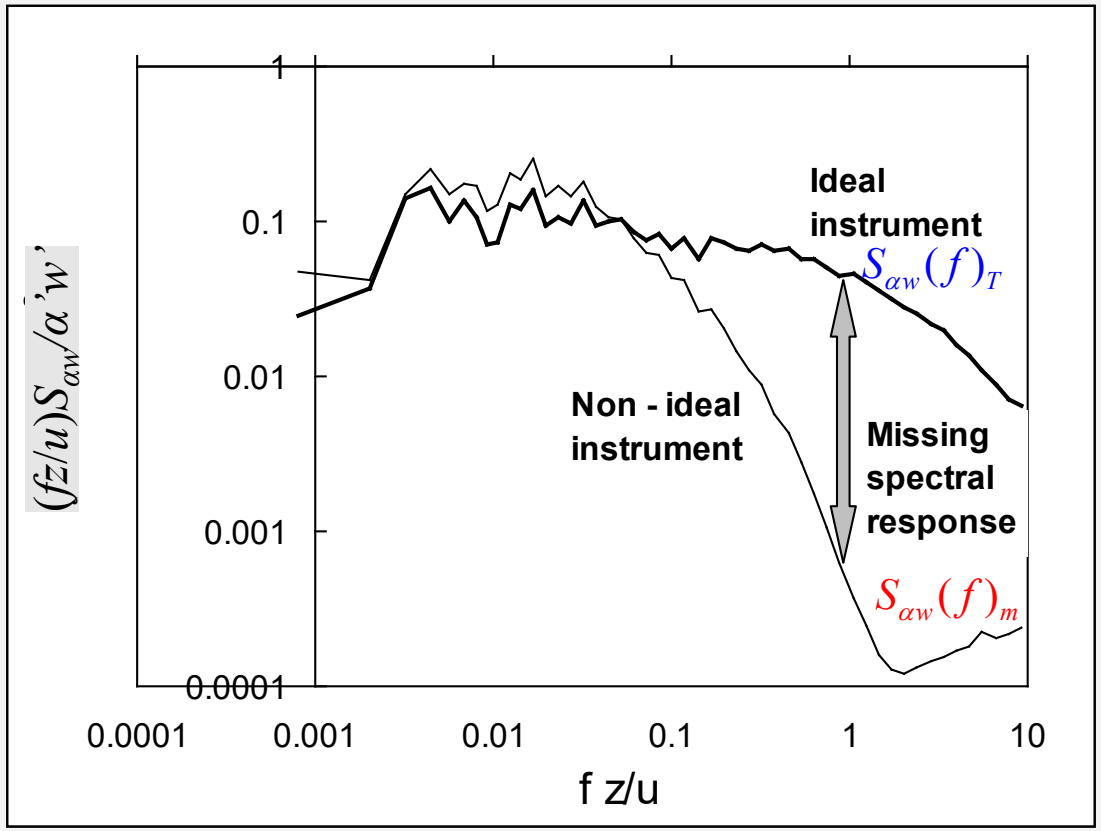

$$\left(\overline{\alpha' w'}\right)_T = \int_0^\infty S_{\alpha w}(f)_T \, df$$

$$\left(\overline{\alpha' w'}\right)_m = \int_0^\infty S_{\alpha w}(f)_m \, df$$

Relate "true" flux to measured flux, measured spectrum, and "true" spectrum

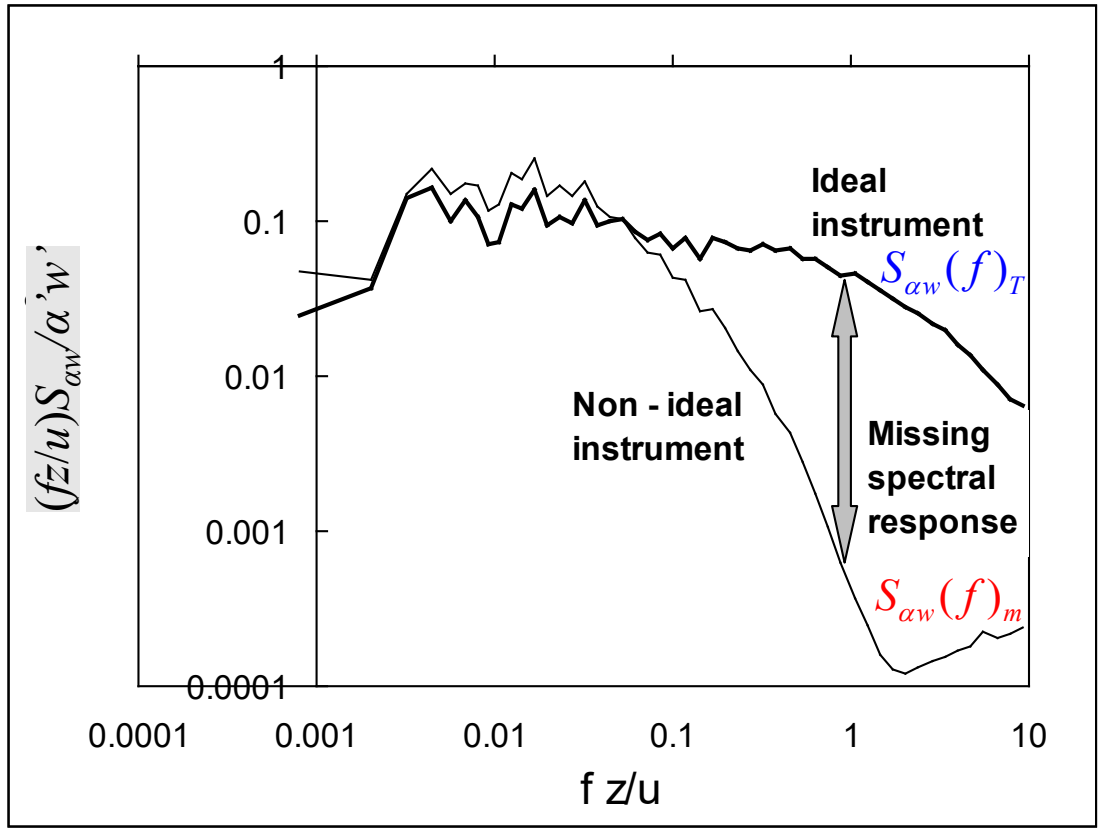

'true' covariance

'true' cospectrum

$$\frac{\left(\overline{\alpha' w'}\right)_T}{\left(\overline{\alpha' w'}\right)_m} = \frac{\int_0^\infty S_{\alpha w}(f)_T \, df}{\int_0^\infty S_{\alpha w}(f)_m \, df}$$

Measured covariance

Measured cospectum

Definition of Transfer Function

$$T_{\alpha w}(f) = \frac{S_{\alpha w}(f)_m}{S_{\alpha w}(f)_T} \leq 1$$

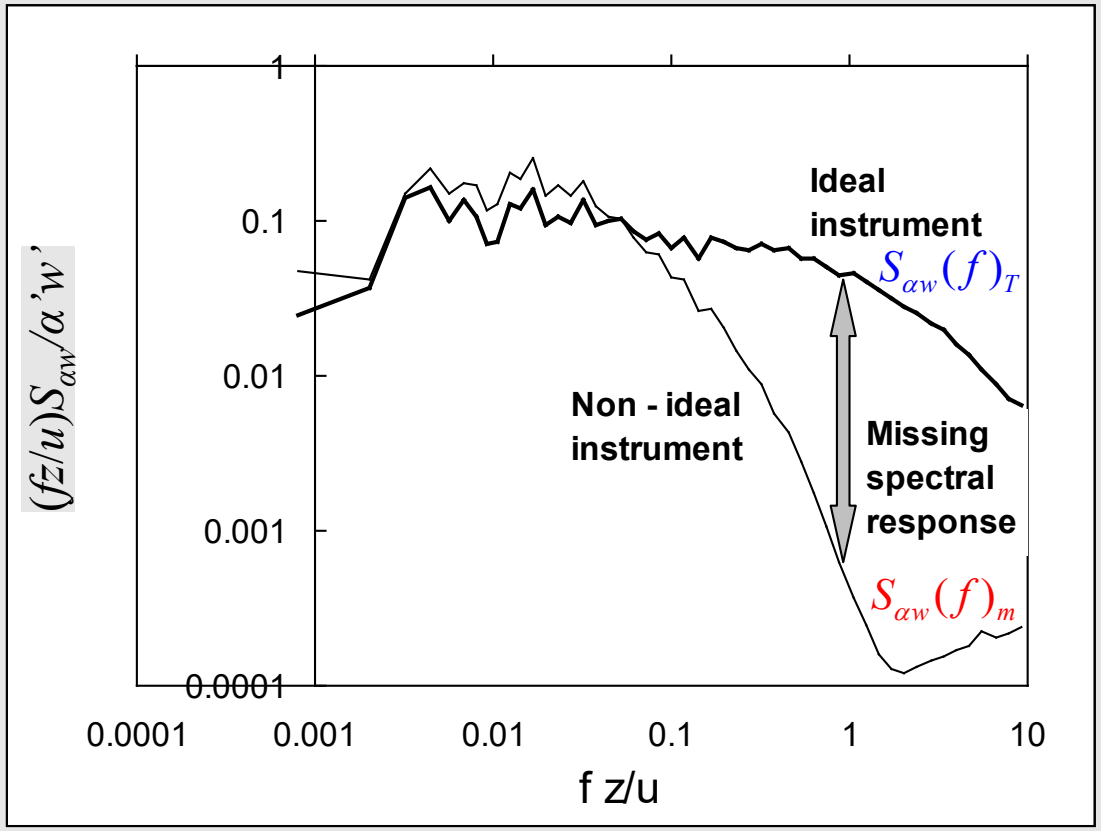

An example for the derivation of transfer function

$$\frac{dT_m(t)}{dt} = \frac{T(t) - T_m(t)}{\tau}$$

Apply Fourier Transform to both sides of this equation

$$\mathcal{F}\left(\frac{dT_m(t)}{dt}\right) = \mathcal{F}\left(\frac{T(t) - T_m(t)}{\tau}\right) \longrightarrow -i\varpi T_m(\varpi) = \frac{1}{\tau}\left[T(\varpi) - T_m(\varpi)\right]$$

$$\sqrt{i} = -1 \qquad \varpi = 2\pi f$$

$$\frac{T_m(2\pi f)}{T(2\pi f)} = \frac{1}{1 - i\tau 2\pi f} = T_T(f)$$

Transfer function

based on spectrum of T

$$T_T(f) = \frac{1}{1 - i2\pi\tau f}$$

based on power spectrum of T

$$T_{TT}(f) = \frac{1}{1 + (2\pi\tau f)^2}$$

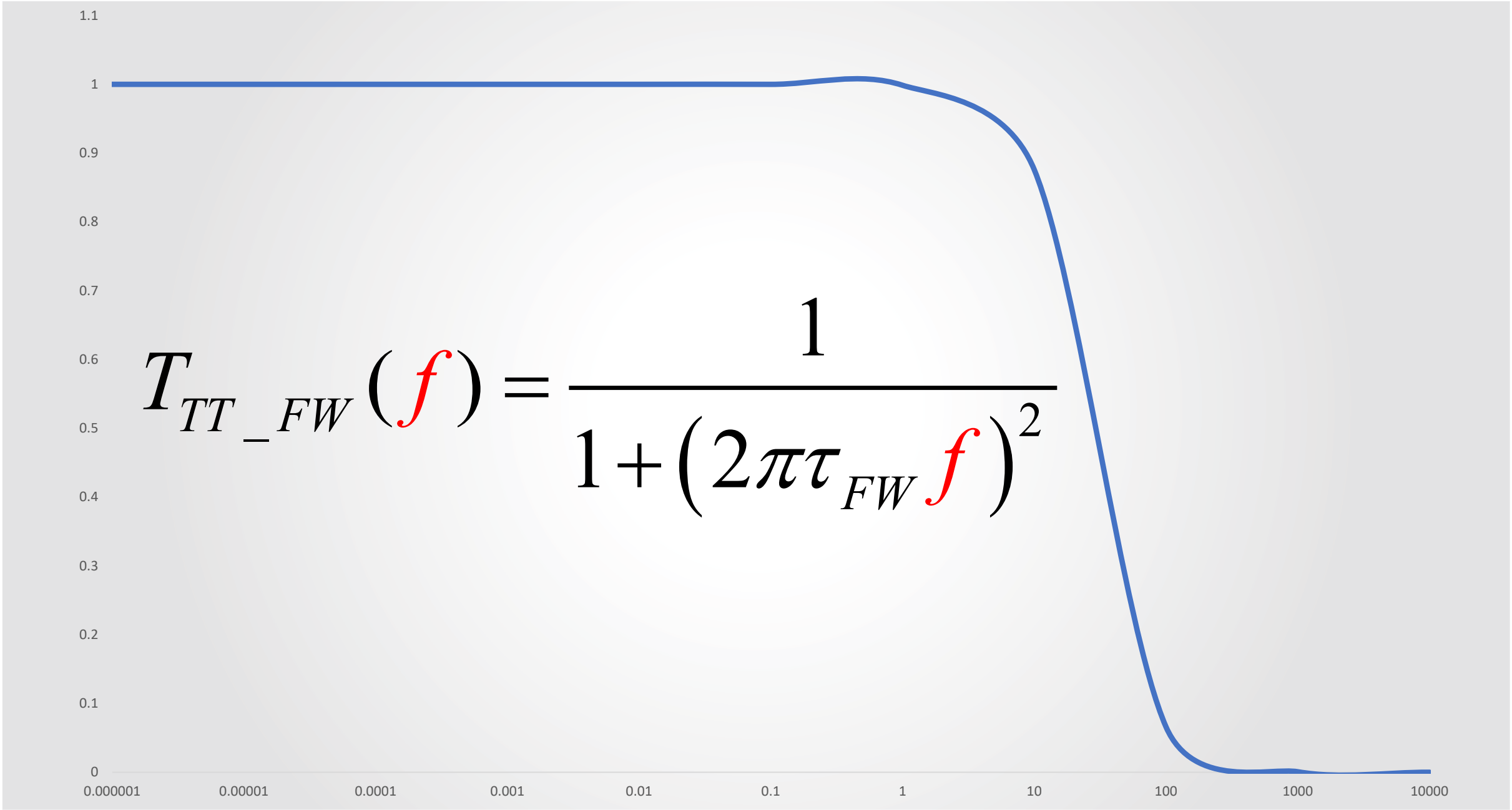
1.1
1
0.9
0.8
0.7
0.6
0.5
0.4
0.3
0.2
0.1
0
0.000001
0.00001
0.0001
0.001
0.01
0.1
1
10
100
1000
10000
$T_{TT\_FW}(f) = \frac{1}{1+(2\pi\tau_{FW} f)^2}$

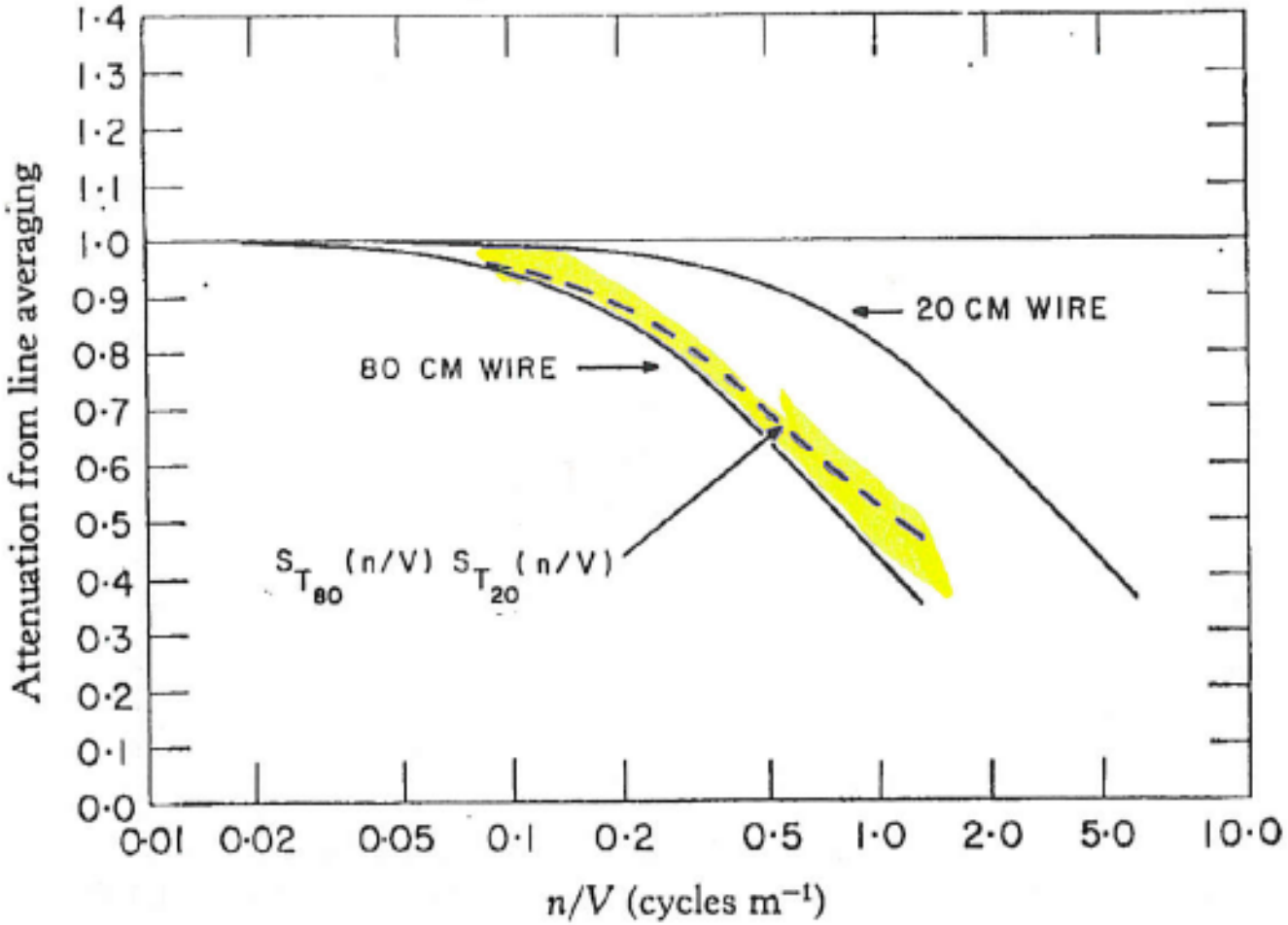

Figure 3. Theoretical attenuation curves for 20- and 80-cm line averaging. Relative attenuation between the two is indicated by dashed curves.

Line averaging

Transfer function for scalars

$$T_{ss\_LA}(f) = \frac{1}{2\pi fp/u}\left(3 + \exp(-2\pi\frac{p}{u}f) - \frac{4\left[1-\exp(-2\pi\frac{p}{u}f)\right]}{2\pi fp/u}\right)$$

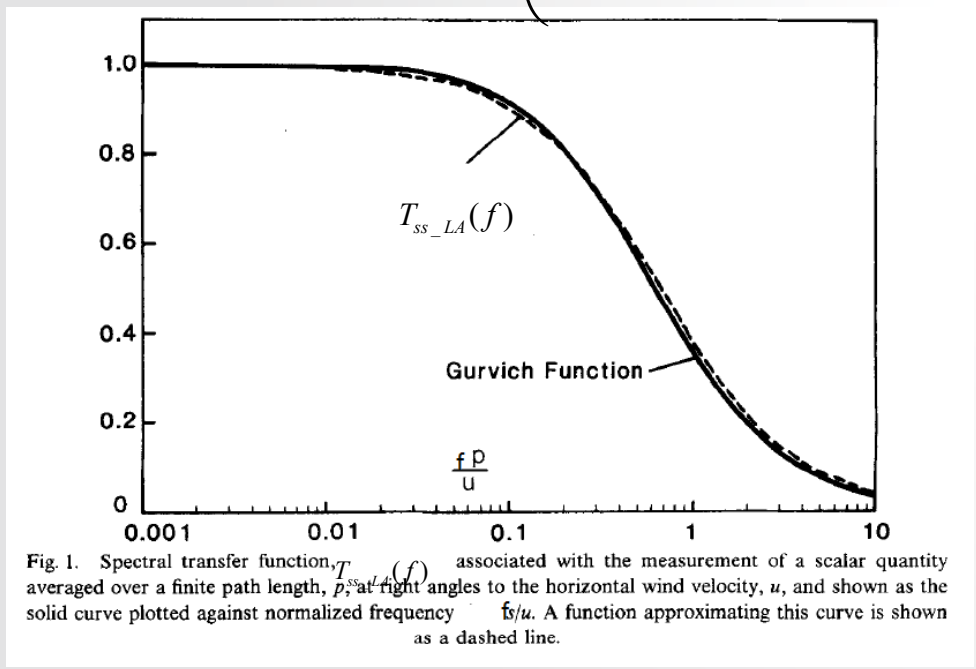

Fig. 1. Spectral transfer function, $T_{ss\_LA}(f)$ associated with the measurement of a scalar quantity averaged over a finite path length, p, at right angles to the horizontal wind velocity, u, and shown as the solid curve plotted against normalized frequency fs/u. A function approximating this curve is shown as a dashed line.

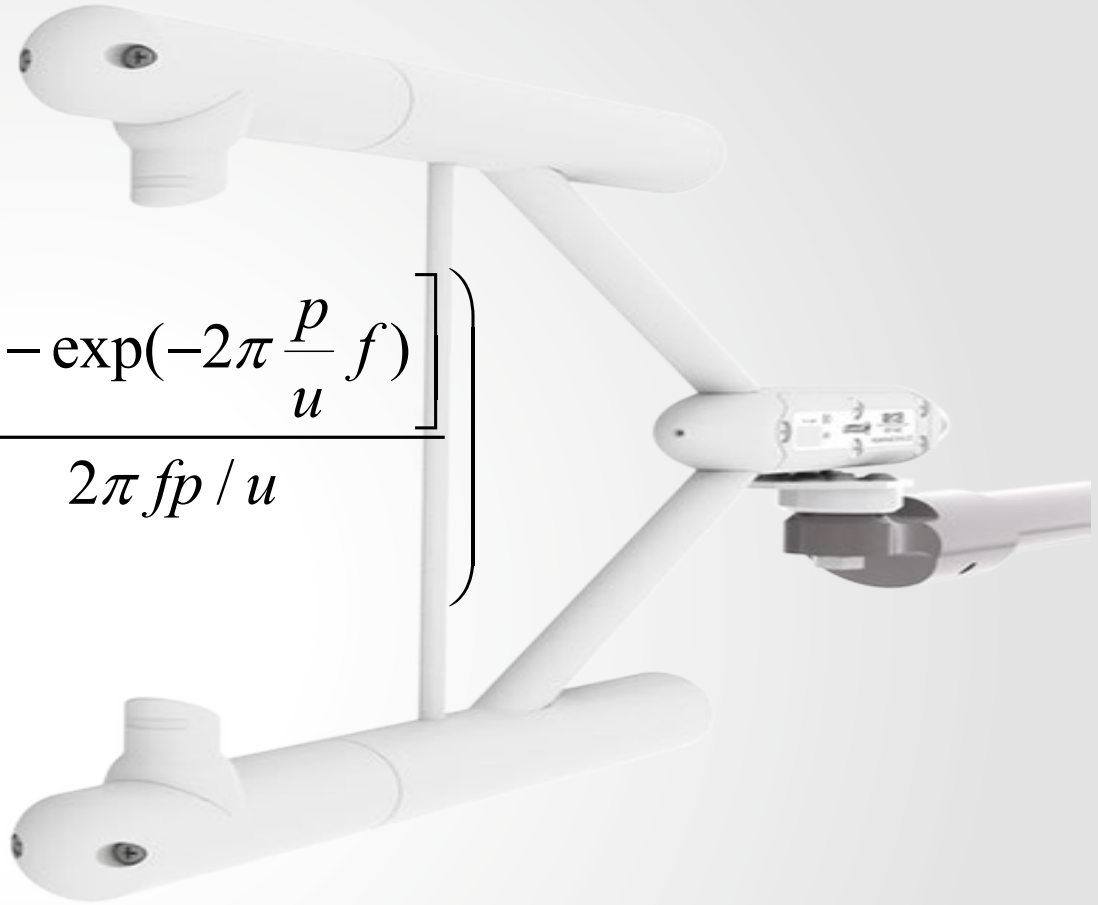

Moore, CJ. 1986. Frequency response corrections for eddy correlation systems, Boundary-Layer Meteorol, 37: 17–35,

Line averaging

Transfer function for vertical wind

$$T_{ww\_LA}(f) = \frac{2}{\pi fp/u}\left(1 + \frac{\exp(-2\pi\frac{p}{u}f)}{2} - \frac{3\left[1-\exp(-2\pi\frac{p}{u}f)\right]}{4\pi fp/u}\right)$$

Moore, CJ. 1986. Frequency response corrections for eddy correlation systems, Boundary-Layer Meteorol, 37: 17–35,

Line averaging

Transfer function for CSAT sonic temperature flux

$$T(k) = \frac{1}{\beta z \overline{w} S(|k|z)^{-7/3}} \int_0^{\infty} \int_0^{2\pi} KA \frac{k^2 + K^2 \sin^2\theta}{\sqrt{k^2 + K^2}} \times \frac{1}{3}\left[\sin c\left(\frac{\mathbf{k}\cdot\mathbf{I}_a}{2}\right) + \sin c\left(\frac{\mathbf{k}\cdot\mathbf{I}_b}{2}\right) + \sin c\left(\frac{\mathbf{k}\cdot\mathbf{I}_c}{2}\right)\right] d\theta dK$$

TABLE 1. Transfer functions for 1D and for 3D sonic anemometers.

kl	1D	3D–30°	3D–45°
0.01	1.0000	1.0000	1.0000
0.1	0.9998	0.9992	0.9990
0.2	0.9980	0.9976	0.9972
0.5	0.9914	0.9900	0.9886
1	0.9720	0.9670	0.9619
1.2	0.9620	0.9550	0.9479
1.4	0.9509	0.9417	0.9325
1.6	0.9390	0.9274	0.9157
1.8	0.9263	0.9122	0.8979
2	0.9130	0.8962	0.8792
2.2	0.8993	0.8797	0.8597
2.4	0.8851	0.8626	0.8397
2.6	0.8707	0.8452	0.8192
2.8	0.8560	0.8274	0.7983
3	0.8412	0.8096	0.7773
4	0.7668	0.7201	0.6720
5	0.6954	0.6353	0.5729
6	0.6296	0.5588	0.4855
7	0.5706	0.4922	0.4117
8	0.5185	0.4355	0.3515
9	0.4728	0.3879	0.3038
10	0.4330	0.3481	0.2664
14	0.3181	0.2445	0.1822
20	0.2241	0.1700	0.1288
30	0.1495	0.1134	0.8580E-01
40	0.1121	0.8503E-01	0.6436E-01
50	0.8968E-01	0.6802E-01	0.5149E-01
60	0.7473E-01	0.5668E-01	0.4291E-01
70	0.6406E-01	0.4859E-01	0.3678E-01
80	0.5605E-01	0.4251E-01	0.3218E-01
90	0.4982E-01	0.3779E-01	0.2860E-01
100	0.4484E-01	0.3401E-01	0.2574E-01

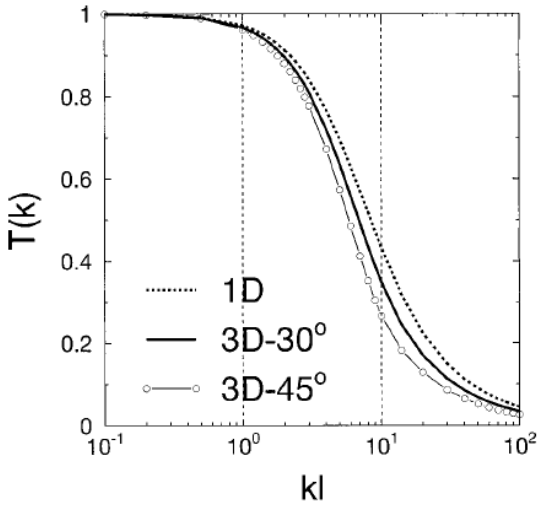

FIG. 3. Transfer functions for sonic anemometers: the dashed line gives the 1D case, the continuous line is for the 3D Campbell–Solent type of sonic and the circles represent a configuration where the acoustic paths make an angle of 45° with the vertical axis. The quantity on the horizontal axis is wavenumber $k \equiv 2\pi/\lambda$ of a flux contribution made dimensionless with acoustic pathlength l.

van Dijk. (2002)

Separation between sensors

Transfer functions for vertical wind with scalar

$$T_{w\_s}(f) = \exp\left[-9.9\left(\frac{f \times d}{\overline{u}}\right)^{1.5}\right]$$

Alternatively, lag maximization

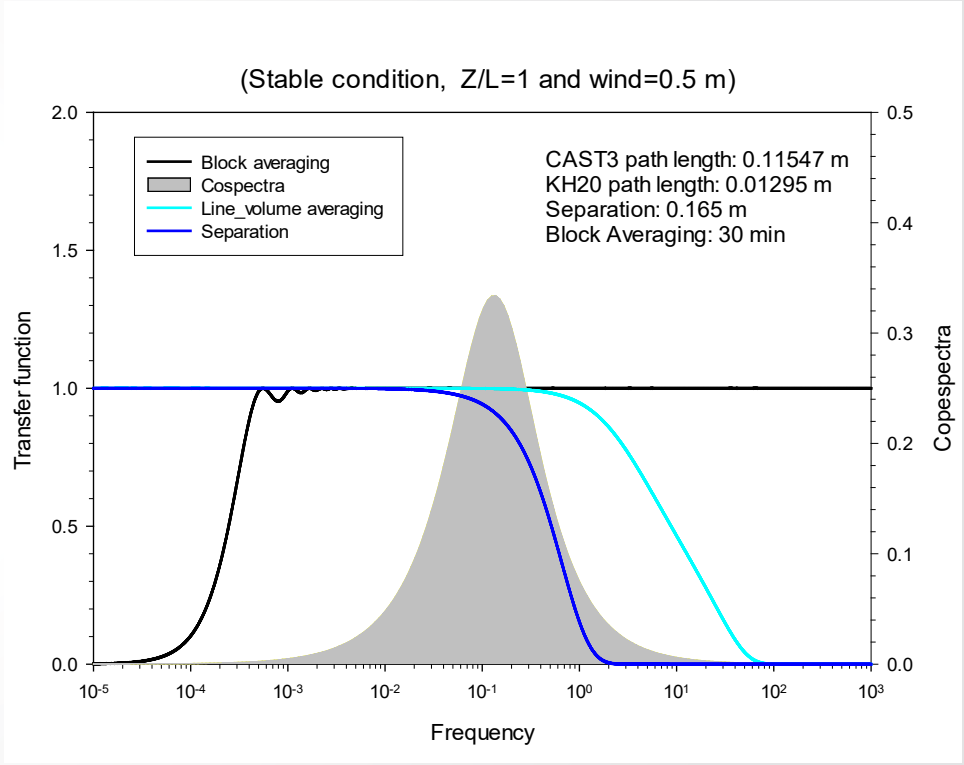

Response delay

Transfer functions for closed-path sampling cell

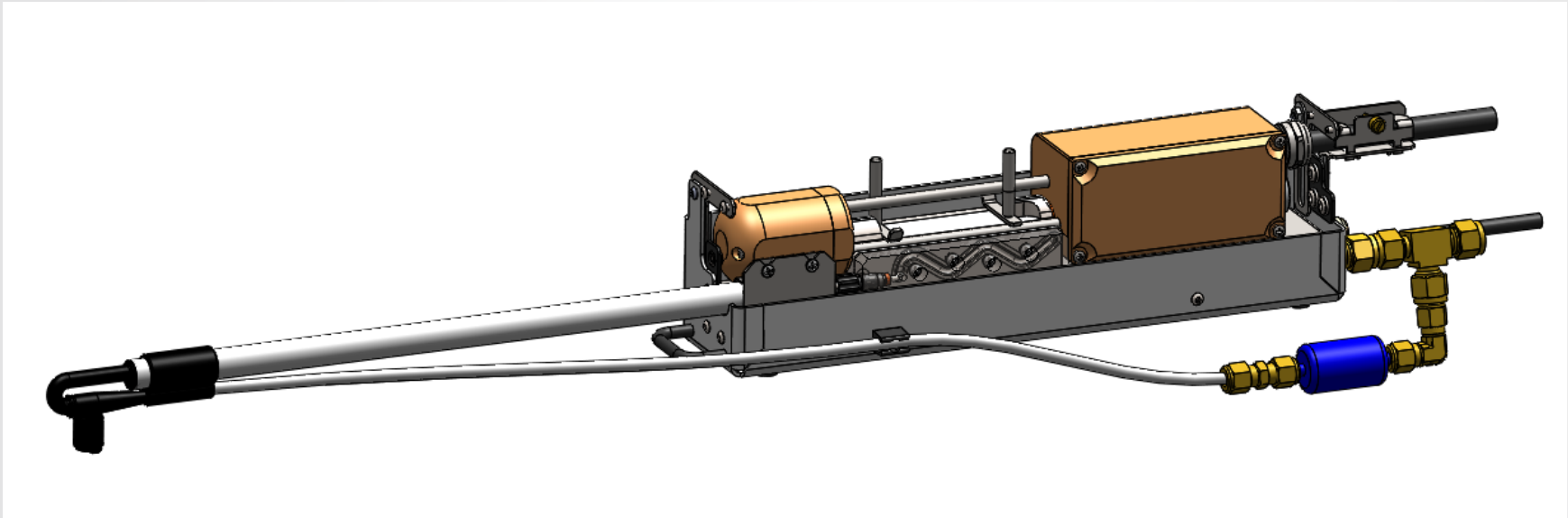

$$T_{CO_2CO_2}(f) = \frac{1}{1+\left(2\pi\frac{f}{4.6}\right)^2}$$

Transfer function

block averaging

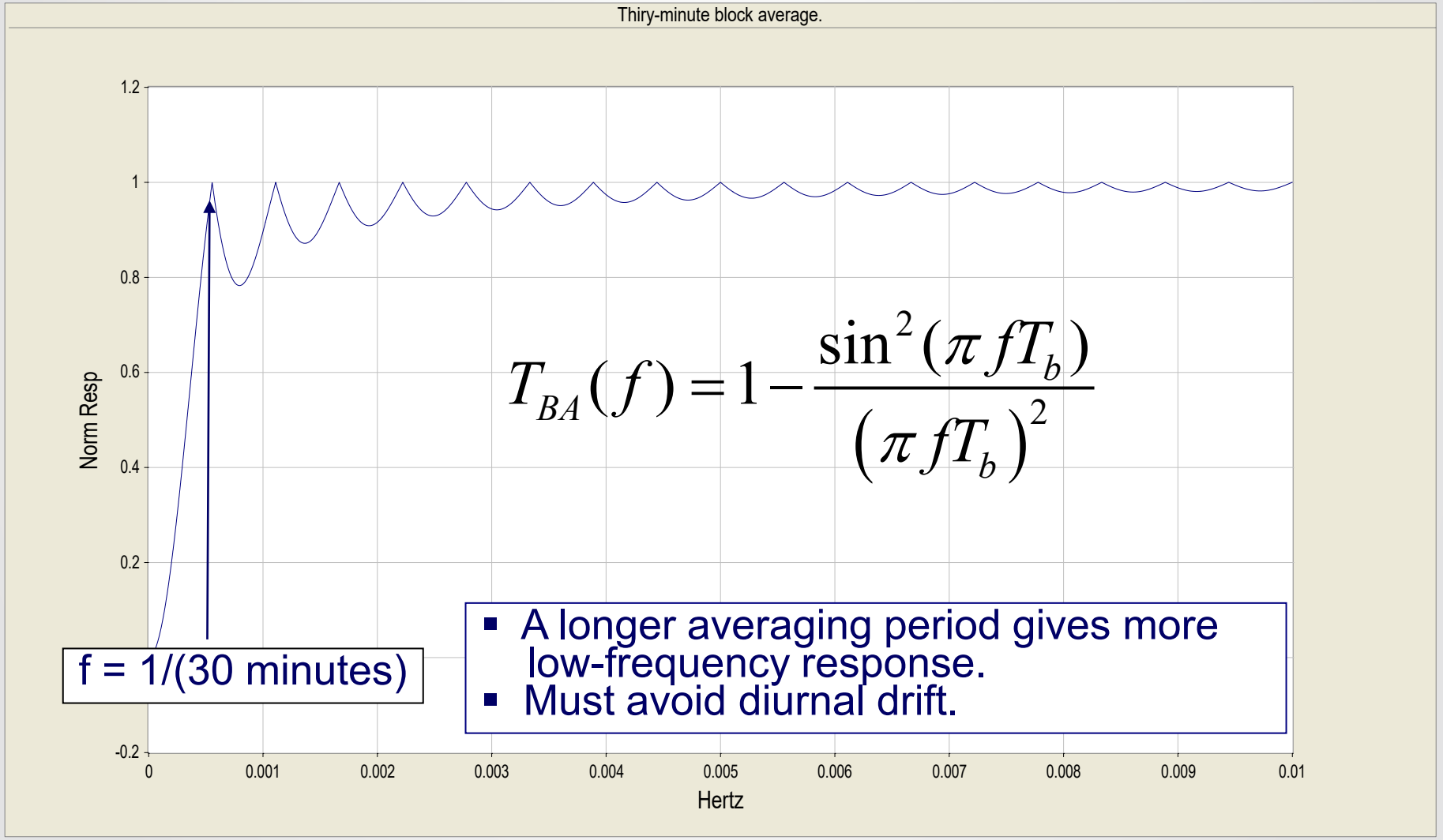

Derivation of measured cospectrum

$$T_{\alpha w}(f) = \frac{S_{\alpha w}(f)_m}{S_{\alpha w}(f)_T} \leq 1$$

$$S_{\alpha w}(f)_m = T_{\alpha w}(f) S_{\alpha w}(f)_T$$

$$S_{\alpha w}(f)_m = T_{\alpha w}(f) S_{\alpha w}(f)_T$$

'true' covariance

'true' cospectrum

$$\frac{\left(\overline{\alpha' w'}\right)_T}{\left(\overline{\alpha' w'}\right)_m} = \frac{\int_0^\infty S_{\alpha w}(f)_T \, df}{\int_0^\infty S_{\alpha w}(f)_m \, df}$$

Measured covariance

Measured cospectum

$$\frac{\left(\overline{\alpha' w'}\right)_T}{\left(\overline{\alpha' w'}\right)_m} = \frac{\int_0^\infty S_{\alpha w}(f)_T \, df}{\int_0^\infty T_{\alpha w}(f) S_{\alpha w}(f)_T \, df}$$

Transfer function

$$\frac{\left(\overline{\alpha' w'}\right)_T}{\left(\overline{\alpha' w'}\right)_m} = \frac{\int_0^\infty S_{\alpha w}(f)_T \, df}{\int_0^\infty T_{\alpha w}(f) S_{\alpha w}(f)_T \, df} = \frac{\int_0^\infty \left[\left(\overline{\alpha' w'}\right)_T S_{\alpha w}(f)_N\right] df}{\int_0^\infty T_{\alpha w}(f) \left[\left(\overline{\alpha' w'}\right)_T S_{\alpha w}(f)_N\right] df}$$

'true' covariance

$$\left(\overline{\alpha' w'}\right)_T = \left(\overline{\alpha' w'}\right)_m \frac{\int_0^\infty S_{\alpha w}(f)_N \, df}{\int_0^\infty T_{\alpha w}(f) S_{\alpha w}(f)_N \, df}$$

Measured covariance

Transfer function

‘true’ covariance

$$\left(\overline{\alpha' w'}\right)_T = \left(\overline{\alpha' w'}\right)_m \frac{\int_0^\infty S_{\alpha w}(f)_N \, df}{\int_0^\infty T_{\alpha w}(f) S_{\alpha w}(f)_N \, df}$$

Measured covariance

Transfer function

Frequency correction factor f_c

$$f_c = \frac{\int_0^\infty S_{\alpha w}(f)_N \, df}{\int_0^\infty T_{\alpha w}(f) S_{\alpha w}(f)_N \, df} \geq 1$$

$$\left(\overline{\alpha' w'}\right)_T = f_c \left(\overline{\alpha' w'}\right)_m$$

Frequency correction factor

$$f_c = \frac{\int_0^\infty S_{\alpha w}(f)_N \, df}{\int_0^\infty T_{\alpha w}(f) S_{\alpha w}(f)_N \, df} \geq 1$$

A product of all transfer functions for related sensors.

$$\left(\overline{\alpha' w'}\right)_T = f_c \left(\overline{\alpha' w'}\right)_m$$

The composite Simpson's rule writes the integration

$$\int_{10^{-6}}^{10000} fS_{\alpha w}(f)_N \, d(\ln f) \approx \frac{\ln \Delta f}{3}\left\{\left[10^{-6} S_{\alpha w}(10^{-6})_N\right] + 4\sum_{k=1}^{50}\left[10^{-6}\Delta f^{2k-1} S_{\alpha w}(10^{-6}\Delta f^{2k-1})_N\right] + 2\sum_{k=1}^{49}\left[10^{-6}\Delta f^{2k} S_{\alpha w}(10^{-6}\Delta f^{2k})_N\right] + \left[10^{4} S_{\alpha w}(10^{4})_N\right]\right\}$$

$$f_c = \frac{\int_{10^{-6}}^{10000} fS_{\alpha w}(f)_N \, d\ln f}{\int_{10^{-6}}^{10000} T_{\alpha w}(f)\left[fS_{\alpha w}(f)_N\right] d\ln f}$$

Burden and Faires (1993)

$$\int_{10^{-6}}^{10000} T_{\alpha w}(f)\left[fS_{\alpha w}(f)_N\right] d(\ln f) \approx \frac{\ln \Delta f}{3}\left\{\left[T_{\alpha w}(10^{-6})10^{-6} S_{\alpha w}(10^{-6})_N\right] + 4\sum_{k=1}^{50} T_{\alpha w}(10^{-6}\Delta f^{2k-1})\left[10^{-6}\Delta f^{2k-1} S_{\alpha w}(10^{-6}\Delta f^{2k-1})_N\right] + 2\sum_{k=1}^{49} T_{\alpha w}(10^{-6}\Delta f^{2k})\left[10^{-6}\Delta f^{2k} S_{\alpha w}(10^{-6}\Delta f^{2k})_N\right] + T_{\alpha w}(10^{4})\left[10^{4} S_{\alpha w}(10^{4})_N\right]\right\}$$

f_c

Correction factors in Flux_notes file for different covariance (i.e., flux)

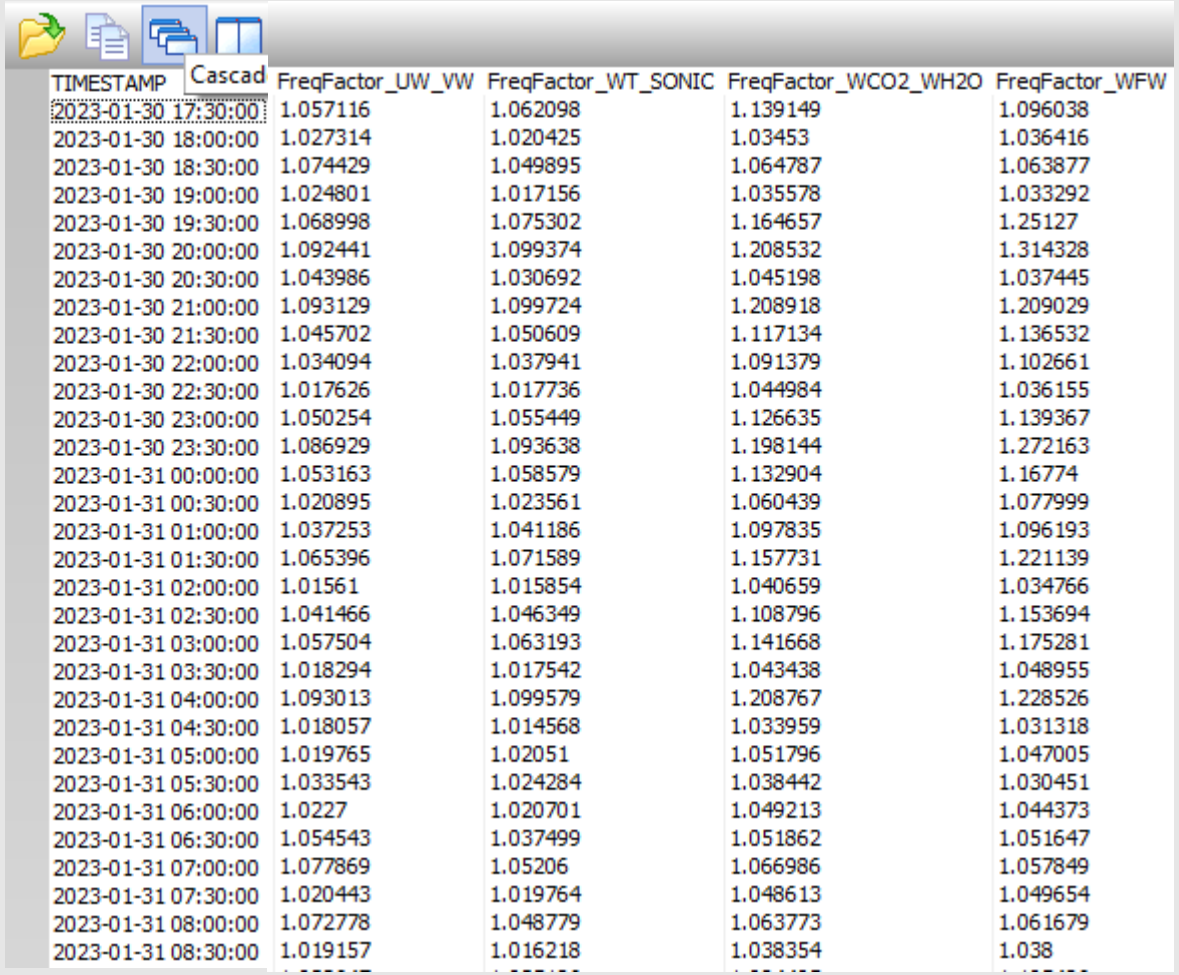

TIMESTAMP	FreqFactor_UW_VW	FreqFactor_WT_SONIC	FreqFactor_WCO2_WH2O	FreqFactor_WFW
2023-01-30 17:30:00	1.057116	1.062098	1.139149	1.096038
2023-01-30 18:00:00	1.027314	1.020425	1.03453	1.036416
2023-01-30 18:30:00	1.074429	1.049895	1.064787	1.063877
2023-01-30 19:00:00	1.024801	1.017156	1.035578	1.033292
2023-01-30 19:30:00	1.068998	1.075302	1.164657	1.25127
2023-01-30 20:00:00	1.092441	1.099374	1.208532	1.314328
2023-01-30 20:30:00	1.043986	1.030692	1.045198	1.037445
2023-01-30 21:00:00	1.093129	1.099724	1.208918	1.209029
2023-01-30 21:30:00	1.045702	1.050609	1.117134	1.136532
2023-01-30 22:00:00	1.034094	1.037941	1.091379	1.102661
2023-01-30 22:30:00	1.017626	1.017736	1.044984	1.036155
2023-01-30 23:00:00	1.050254	1.055449	1.126635	1.139367
2023-01-30 23:30:00	1.086929	1.093638	1.198144	1.272163
2023-01-31 00:00:00	1.053163	1.058579	1.132904	1.16774
2023-01-31 00:30:00	1.020895	1.023561	1.060439	1.077999
2023-01-31 01:00:00	1.037253	1.041186	1.097835	1.096193
2023-01-31 01:30:00	1.065396	1.071589	1.157731	1.221139
2023-01-31 02:00:00	1.01561	1.015854	1.040659	1.034766
2023-01-31 02:30:00	1.041466	1.046349	1.108796	1.153694
2023-01-31 03:00:00	1.057504	1.063193	1.141668	1.175281
2023-01-31 03:30:00	1.018294	1.017542	1.043438	1.048955
2023-01-31 04:00:00	1.093013	1.099579	1.208767	1.228526
2023-01-31 04:30:00	1.018057	1.014568	1.033959	1.031318
2023-01-31 05:00:00	1.019765	1.02051	1.051796	1.047005
2023-01-31 05:30:00	1.033543	1.024284	1.038442	1.030451
2023-01-31 06:00:00	1.0227	1.020701	1.049213	1.044373
2023-01-31 06:30:00	1.054543	1.037499	1.051862	1.051647
2023-01-31 07:00:00	1.077869	1.05206	1.066986	1.057849
2023-01-31 07:30:00	1.020443	1.019764	1.048613	1.049654
2023-01-31 08:00:00	1.072778	1.048779	1.063773	1.061679
2023-01-31 08:30:00	1.019157	1.016218	1.038354	1.038

Primary references

Kaimal, JC 1968. The effect of vertical line averaging on the spectra of temperature and heat-flux, Qaurt. J. Roy. Meteor. Soc. 94: 149-155.

Kaimal, JC, SF Clifford, RJ Lataitis. 1989. Effect of finite sampling on atmospheric spectra. Bound-Layer Meteorol 7: 827-837.

Kaimal, J C, J J Finnigan. 1994. Atmospheric Boundary Layer Flows: Their Structure and Measurement. Oxford University Press, Oxford, 289 p.

Kaimal, JC, JC, Wyngaard, Y Izumi, OR Cote. 1972. Deriving power spectra from a three-component sonic anemometer. J Appl Meteorol 7: 827-837.

Kaimal, JC, JC, Wyngaard, Y Izumi, OR Cote. 1972. Spectral characteristics of surface-layer turbulence. Qurt J R Met Soc 98: 563-589.

Moore CJ. 1986. Frequency response corrections for eddy correlation systems. Bound-Layer Meteorol 37: 17-35.

van Dijk, A. 2002a. Extension of 3D of "the effect of linear averaging on scalar flux measurements with a sonic anemometer near the surface" by Kristensen and Fitzjarrald. J Atm Ocean Techn. 19: 80-19.

Secondary references

Horst, TW, 1997. A simple formula for attenuation of eddy fluxes measured with first-order response scalar sensors. Bound-Layer Meteorol 94: 517-520.

Massman, WJ. 2000. A simple method for estimating frequency response corrections for eddy covariance systems. Agr For Meteorol 104: 185-198.

Moncrieff, JB, JM Massheder, H.de Bruin, JA Elbers, T Friborg, B Heusinkveld, P Kabat, S Scott, H Soegaard, A Verhoef. 1997. A system to measure surface fluxes of momentum, sensible heat, water vapour and carbon dioxide. J of Hydrology 188-189: 589-611.

van Dijk, A. 2002b. The Principle of Surface Flux Physics. Research Group of the Royal Netherlands Meteorological Institute and Department of Meteorology and Air Quality with Agricultural University Wageningen. 65p.

Closed-path reference

Fratini, G, A. Ibrome, N Arrga, G. Burba, D. Papale. 2012. Relative humidity effect on water vapor fluxes measured with closed-path eddy-covariance system with short sampling line. Agr For Meteorol 165: 53-63.

Ibrom, A, E Dellwik, H Flyvbjerg, NO Jensen, K Pilegaard. 2007. Strong low-pass filtering effects on water vapour flux measurements with closed-path eddy correlation systems, Agr Forest Meteorol 147:140–156.

Other references

Andreas, EL. 1981. The effects of volume averaging on spectra measured with Lyman-Alpha hygrometer. J App Meteorol 20: 467-475.

Burden, RL and J.D. Faires. 1993. Numerical Analysis. PWS Publishing Company, Boston. pp. 184-189.

Horst, T W, DH Lenschow. 2009. Attenuation of scalar fluxes measured with spatially-displaced sensors, Boundary-Layer Meteorology, 130, 275–300.

Leuning, R, KM King. 1992. Comparison of eddy-covariance measurements of CO_2 flux by open- and close-path CO_2 Analyzers. Bound-Layer Meteorol 59: 297-311.

Laubach, J, KG, McNaughton. 1998. A spectrum-independent procedure for correcting eddy flux measured with separated sensors. Bound-Layer Meteorol 89: 445-467.

Lumley, JL, H.A. Panofsky. 1964. The Structure of Atmospheric Turbulence. John Wiley & Son, New York, 239 p.

Moene, AF. 2003. Effects of water vapor on the structure parameter of the refractive index for near-infrared radiation. Bound-Layer Meteorol 107: 635-653.

Shapland, TM, RL Snyder, KT Paw U, AJ McElrone. 2014. Thermocouple frequency response compensation leads to convergence of the surface renewal alpha calibration. Agricul For Meteorol 189-190: 36-47.


Questions?